Regime-dependent forecast uncertainty of convective precipitation

CHRISTIAN KEIL* and GEORGE C. CRAIG

Meteorologisches Institut Ludwig-Maximilians-Universität, München, Germany

Abstract

Forecast uncertainty of convective precipitation is influenced by all scales, but in different ways in different meteorological situations. Forecasts of the high resolution ensemble prediction system COSMO-DE-EPS of Deutscher Wetterdienst (DWD) are used to examine the dominant sources of uncertainty of convective precipitation. A validation with radar data using traditional as well as spatial verification measures highlights differences in precipitation forecast performance in differing weather regimes. When the forecast uncertainty can primarily be associated with local, small-scale processes individual members run with the same variation of the physical parameterisation driven by different global models outperform all other ensemble members. In contrast when the precipitation is governed by the large-scale flow all ensemble members perform similarly. Application of the convective adjustment time scale confirms this separation and shows a regime-dependent forecast uncertainty of convective precipitation.

Zusammenfassung

Generell wird die Vorhersagbarkeit konvektiven Niederschlags von Prozessen auf allen Skalen beeinflusst. Im Einzelfall hängt diese aber entscheidend von der meteorologischen Strömungssituation ab. Verschiedene Ursachen der Vorhersagbarkeit, bzw. der Ungenauigkeit der Vorhersage, lassen sich mit Vorhersagen des konvektions-auflösenden Ensemble-Vorhersage-Systems COSMO-DE-EPS des Deutschen Wetterdienstes (DWD) untersuchen. Eine Überprüfung der Vorhersagequalität mit traditionellen und räumlichen Qualitäts-maßen angewandt auf Radarbeobachtungen verdeutlicht die unterschiedliche Güte der Niederschlagsprog-nosen während verschiedener meteorologischer Strömungssituationen. Falls die Vorhersagbarkeit in erster Linie von klein-skaligen Prozessen beeinflusst wird, haben diejenigen Vorhersagen eine höhere Qualität, die mit derselben physikalischen Störung aber verschiedenen globalen Modellen angetrieben werden. Falls der Niederschlag von der synoptisch-skaligen Strömung dominiert wird, zeigen alle Vorhersagen eine ähnliche Qualität. Die Anwendung der konvektiven Zeitskala bestätigt diese Unterteilung und zeigt die strömungsabhängige Vorhersagbarkeit des konvektiven Niederschlags.

1 Introduction

The improvement of quantitative precipitation forecasts (QPF) is one of the key challenges in numerical weather prediction (NWP). The increase in model resolution to a few kilometres allows an explicit treatment of moist convective processes in place of convective parameter-isations (MOLINARI and DUDEK, 1992) and a better representation of topography and surface fields. It is hoped that convection-permitting models will improve the forecast skill associated with smaller-scale phenom-ena, such as moist convection, and more generally of QPF (EBERT et al., 2003).

On the other hand, the application of short-range convection-permitting models calls for an examination of predictability of the simulated small-scale atmo-spheric phenomena, since the time scale of atmospheric instabilities is related to their spatial scales, and small-scale instabilities grow much faster than those with

larger scales (KALNAY, 2003). Convection is a typi-cal example of a short time scale phenomenon: cumu-lus clouds grow with an exponential time scale of the order of 10 minutes or so. It is therefore impossible to predict the precipitation associated with an individ-ual thunderstorm for more than about an hour. Never-theless, if convective activity is organized or forced by larger scales, then convective precipitation can remain predictable much longer than individual thunderstorms.

Predictability, or forecast uncertainty, can be ad-dressed with ensemble techniques (KALNAY, 2003). While ensemble prediction systems (EPS) are well es-tablished at synoptic-scale medium range weather fore-casts (see. e.g. MOLTENI et al., 1996; LEUTBECHER and PALMER, 2008), the design of short-range convection-permitting EPS is difficult due to the poor knowledge of the mechanisms promoting rapid error growth, the var-ious sources of uncertainty and limited computing re-sources (KONG et al., 2006). Recently, a first step to-wards a convection-permitting EPS (employing a hori-zontal grid spacing of 2.8 km) was done at Deutscher Wetterdienst (DWD) by following a multi-boundary and multi-parameter approach taking into account uncertain-

*Corresponding author: Christian Keil, Meteorologisches Institut, Ludwig-Maximilians-Universität, München, Germany, e-mail: Christian.Keil@lmu.de

Table 1: List of parameters perturbed in COSMO-DE-EPS in 2007. The entrainment rate describes the lateral transport across cloud boundaries via turbulent exchange of mass and influences the moisture budget in the boundary layer. The subgrid-scale cloud cover influences the vertical transport through the production of turbulent kinetic energy and may change the triggering of convection. The scaling factor of the laminar sublayers influences the surface fluxes of moisture and temperature affecting the coupling of the two compartments soil atmosphere. The mixing length influences the dissipation, the vertical transport, the vertical gradients and, eventually, the stability of the atmosphere.

parameter	description	perturbed	default
entr_scv	entrainment rate of shallow convection	0.002	0.0003
clc_diag	subscale cloud cover given grid-scale saturation in the turbulence scheme	0.5	0.75
rlam_heat	scaling factor of the laminar sublayers for scalars	50	1.0
rlam_heat	scaling factor of the laminar sublayers for scalars	0.1	1.0
tur_len	asymptotic mixing length of turbulence scheme	150	500

ties in the lateral boundary conditions and model physics (GEBHARDT et al., 2010).

Forecast uncertainty of convective precipitation is influenced by all scales, but in different ways in different meteorological situations. JONES et al. (2007) performed a careful evaluation of a mesoscale, short-range ensemble forecast system (horizontal grid spacing 12 km) over the northeast of the United States, concentrating on the prediction skill of temperature, wind and precipitation. They found ensemble members based on varied model physics to be more important under weak large-scale forcing of upward motion, whereas a range of initial conditions proved decisive with strong large-scale forcing. DONE et al. (2006) investigated the dynamical role of the synoptic and mesoscale environment in controlling the local characteristics of convective precipitation and proposed two different regimes. During forced (or equilibrium) convection the amount of precipitation is controlled by the large-scale production of Convective Available Potential Energy (CAPE). While the precise local variability of precipitation is unpredictable, the overall size, location and intensity of the precipitating region is determined by the synoptic-scale flow (c.f. ARAKAWA and SCHUBERT, 1974). In the second, local-forced (or non-equilibrium) regime, CAPE is available, but the extent to which it produces convection and precipitation is restricted by the availability of triggers sufficient to overcome a convective inhibition energy (CIN). Triggers include boundary layer convergence regions or local maxima in temperature or moisture. Since these are typically driven by local orographic or surface flux variability, they may be hard to predict, even if the large-scale meteorological situation is known.

DONE et al. (2006) suggested that these distinct meteorological regimes can be identified by considering a time scale of convective adjustment τ_c. This scale (defined in section 2.2, below) is an estimate of the rate at which CAPE is being consumed by convective heating. If the convective time scale is only a few hours, and thus short compared to the time scale over which the large-scale environment evolves (say 1 day) the convection

will remove CAPE as fast as it is created, and the rate of creation of CAPE controls the amount of convection. On the other hand, if the convective time scale is similar to, or longer than, 1 day, convection is acting too slowly to remove the CAPE, and there must be local factors controlling its rate. A climatological study (ZIMMER et al., 2011) has shown that about 60 % of the warm season convective events in Central Europe are synoptically forced.

The goal of this study is to identify a regime-dependent forecast uncertainty of convective precipitation using the convection-permitting COSMO-DE-EPS covering a 9 day period during the COPS field campaign (Convective and Orographically induced Precipitation Study, WULFMEYER et al., 2008). Our hypothesis is that forced-frontal convective precipitation associated with synoptic weather patterns may be predictable for several days and is primarily governed by lateral boundary conditions in limited area models. In contrast, single convective cells developing during air-mass convection situations, which of themselves are predictable only for a matter of hours, are frequently triggered by local, small-scale processes enforced e.g. by mountain ridges and are anticipated to react sensitively to changes in the model physics.

The structure of the paper is as follows. In the next section the convection-permitting ensemble prediction system, the observational data, the quality measures and the definition of the convective adjustment time scale are described. This is followed by the results section before the conclusions are drawn in the final section.

2   Tools and ingredient

2.1   The convection-permitting ensemble

The high resolution ensemble prediction system COSMO-DE-EPS is based on the operational, deterministic COSMO-DE model (BALDAUF et al., 2006) with a horizontal resolution of 2.8 km and 50 vertical levels up to 30 hPa. It is put in ensemble mode by combining lateral boundary conditions of four different global models with five variations of physical parameterizations for
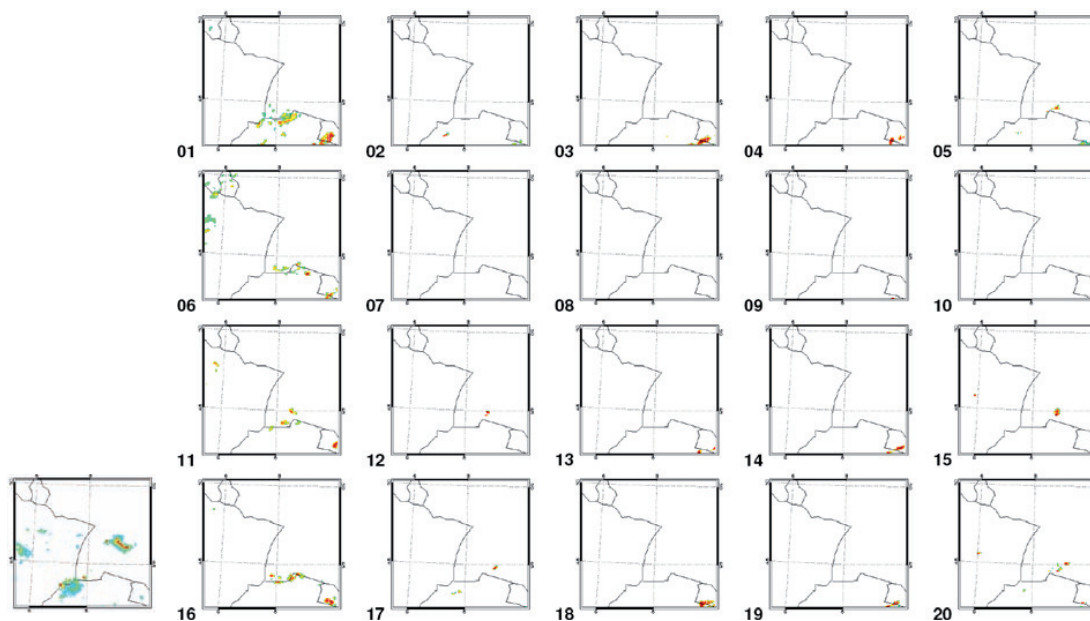
Figure 1: Radar observation (bottom left) and stamp map of forecast synthetic radar imagery displaying all 20 members of COSMO-DE-EPS on 12 August 2007 at 1715 UTC (radar reflectivities 7, 19, 28, 37, 46 and 55 dBZ are color-coded).
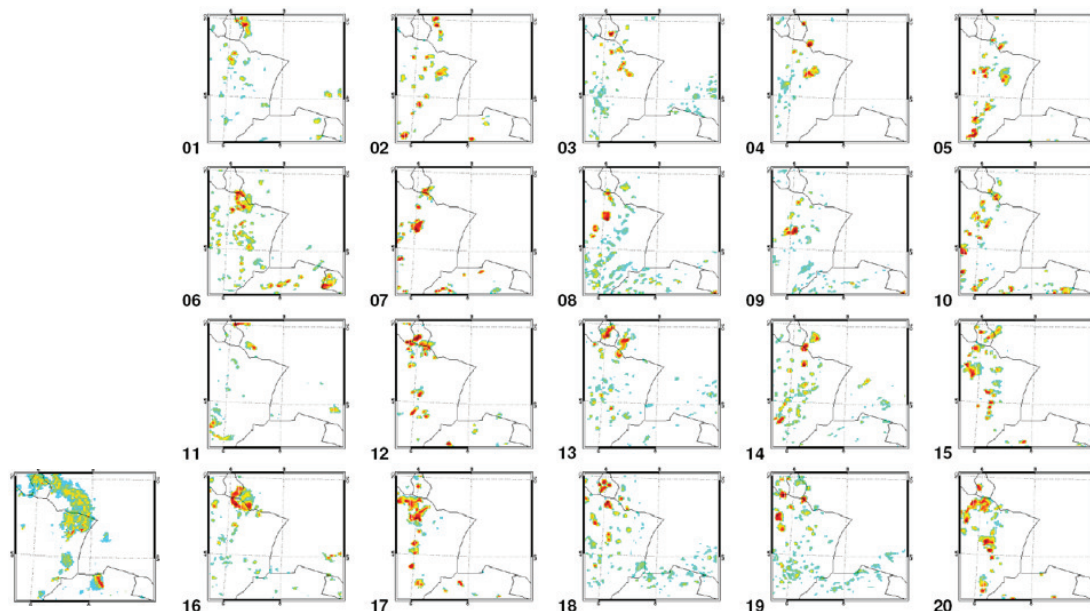

Figure 2: Same as Fig. 1 but at 2315 UTC.

a total of 20 ensemble member forecasts (GEBHARDT, 2010). The different lateral boundary conditions stem form the COSMO-SREPS ensemble (MARSIGLI et al., 2008) and comprise the global models of the European Centre for Medium Range Weather Forecast (ECMWF, members 1–5), the GME model of DWD (members 6-10), the GFS system of the National Center of Environmental Prediction (NCEP, members 11–15) and the Unified Model of the UK MetOffice (members 16–20). The five physics perturbations are accomplished in a non-stochastic and uniform approach by varying exactly

one parameter for each perturbation (Table 1). These parameters are chosen to maximize the variability of convective precipitation. The COSMO-DE-EPS is started daily at 00 UTC with a forecast range of 24 hours. Note that COSMO-DE-EPS was experimental in 2007 and the setup used for this study does not represent the current status.

Here COSMO-DE-EPS fields of synthetic radar reflectivity at 850 hPa pressure surface are used as a proxy for precipitation intensities and to assess forecast quality employing radar observations. In COSMO-DE syn-
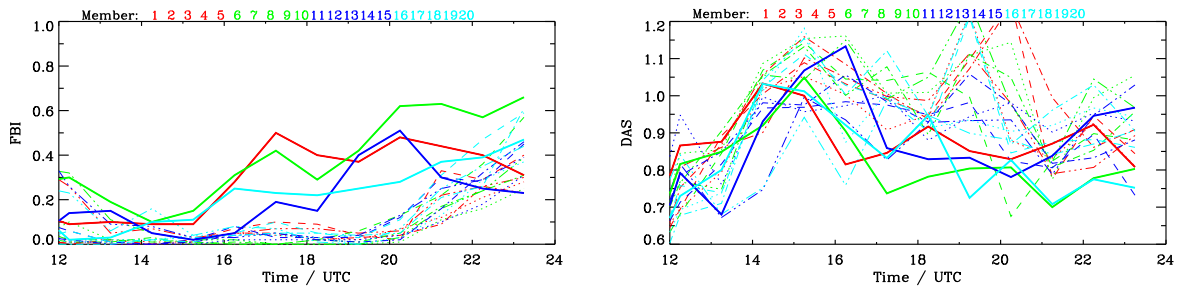
Figure 3: Scores FBI (left) and DAS (right) for all ensemble members applying a threshold of 19 dBZ on 12 August 2007. Different colours depict different driving global models, solid lines members 1, 6, 11 and 16 with changed entrainment rate.
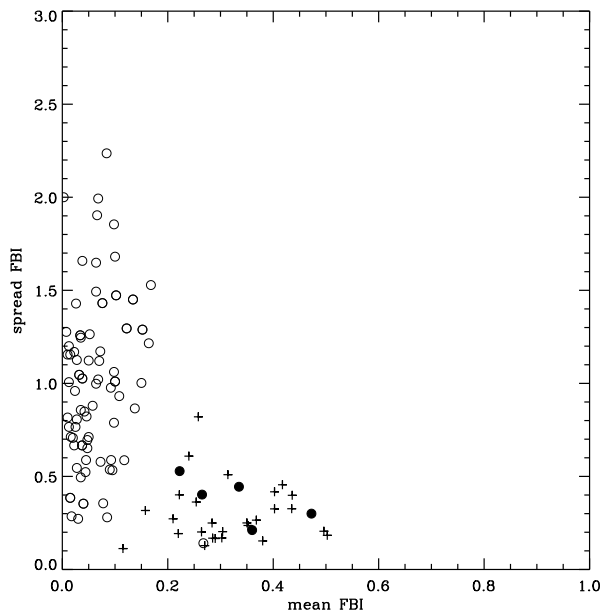

Figure 4: Scatter plot of the mean FBI (any symbol is the average over the same driving model or the same physical perturbation) versus its spread FBI stratified by time. The open circles denote the values for the period from 1215 to 2115 UTC on 12 August, while the plus signs represent the values from 2215 to 2315 UTC. Highlighted (filled circles) is the mean FBI and its spread for the members 1, 6, 11, and 16 (first column in Fig. 1) between 1715 and 2115 UTC (cmp. to Fig. 3).

thetic reflectivities are calculated with a forward operator using information from the hydrometeor distribution of rain, snow and graupel at every grid point. The forecast quality is computed hourly 15 minutes after the full hour due to data availability.

2.2 Observation data and quality measures

Forecast quality is validated using hourly instantaneous radar data of the European Composite. It is provided by DWD and covers an area of 1800 km x 1800 km over Europe. Here, a subdomain of southwestern Germany

and northeastern France centered over the COPS observation region is evaluated. The European radar composite delivers instantaneous radar intensities given in six reflectivity classes (7, 19, 28, 37, 46, 55 dBZ) on a horizontal grid with a resolution of 2 km x 2 km.

The conventional score frequency BIAS (FBI; WILKS, 2006) is used to provide an integral estimate of the model's behaviour in over- or underpredicting rainfall. To exploit the spatial information of the radar data the verification measure DAS (Displacement and Amplitude Score; KEIL and CRAIG, 2009) is applied. DAS is based on an optical flow algorithm that defines a vector field that deforms, or morphs, one image to match the other. In DAS distance and amplitude errors are combined to produce a single measure. Note that the overall performance of DAS is shown in more detail for the same region and time period in a companion article of WEUSTHOFF et al. (2011).

2.3 The convective time scale

The convective adjustment time scale used in this study is defined by DONE et al. (2006). Firstly, the rate of change of CAPE due to release of latent heat is estimated from the rainfall rate by the following formula:

$$\frac{dCAPE}{dt} = \frac{1}{3600} \cdot \frac{L_v}{c_p} \frac{g}{\rho_0 T_0} P$$

P is the precipitation rate (mm/h), L_v the latent heat of vapourisation, g the acceleration due to gravity, c_p the specific heat of air at constant pressure, and T_0 and ρ_0 are reference values of temperature and density, respectively. The convective time scale τ_c can then estimated as

$$\tau_c = \frac{CAPE}{\frac{dCAPE}{dt}} = \frac{1}{2} \frac{c_p}{L_v} \frac{\rho_0 T_0}{g} \frac{CAPE}{P}$$

This is likely to be an overestimation of the convective time scale, since it is based on a pseudo-adiabatic CAPE calculation that ignores entrainment, water loading and feedbacks on the subcloud layer by convective downdrafts. To account for such effects a scaling factor of 1/2 is introduced.
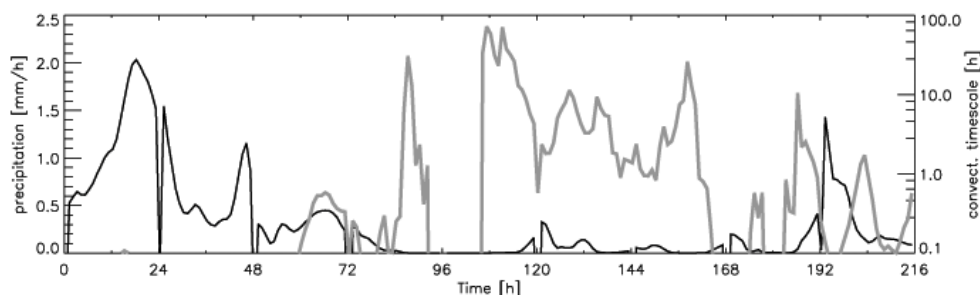
Figure 5: Time series of the ensemble mean precipitation (black line) and the mean convective time scale (grey) averaged over the COPS domain shown in Fig. 1 for the entire period from 8 to 16 August 2007.

A threshold value of convective time scale τ_c must be identified to distinguish between equilibrium and non-equilibrium convection. DONE et al. (2006) suggest a typical synoptic time scale would be a day or more. Over land, changes in forcing associated with the diurnal cycle are likely to be important, so a shorter threshold time scale of around 6 hours is used in this study (as in MOLINI et al., 2011). The exact choice of a threshold value is somewhat arbitrary, but ZIMMER et al. (2011) show that any value in the range 3–12 hours is sufficient to unambiguously classify the majority of cases.

3   Results

Forecasts of COSMO-DE-EPS are continuously available from 8 to 16 August 2007 covering various meteorological situations during the COPS field experiment. First we focus on the meteorological conditions during IOP15 on 12 August and inspect the forecast performance of the ensemble members as seen by stamp maps and two scores highlighting the different flow regimes that day. This is followed by an examination of the entire period applying the convective adjustment time scale to identify regime-dependent forecast uncertainty.

In the afternoon of 12 August local convection triggered by orography occurred over the Swiss Jura, the Vosges and the Black forest mountains in the COPS region. At 1715 UTC a strong convective storm (exceeding 46 dBZ) moved eastward across Stuttgart and two less intense rainfall areas were detected by radar over Switzerland and France (Fig. 1). In contrast to observations, the convective-scale ensemble seems, at first glance, to miss the convective development completely. However, a closer inspection reveals that the ensemble members 1, 6, 11 and 16 outperform the other members by generating some convective precipitation along the Swiss-German border at 1715 UTC (Fig. 1). Recall that these four members are driven by different global models but are run with the same physics perturbation, namely a modified entrainment rate (Table 1). Thus the precipitation forecast seems to be very sensitive to small changes in the physical parameterization and, consequently, exhibit a large forecast uncertainty.

Later that day precipitation along a cold front affected the region. At 2315 UTC radar observations depict a fairly coherent rainfall area crossing the French-German border (Fig. 2). Now, all ensemble members predict precipitation, however, it is spottier, more intense and not correctly located. It seems that the driving global models determine the position of the cold front (lines in Fig. 2), while the structure is mostly governed by the physics perturbation (rows in Fig. 2). Overall, this synoptically forced precipitation is forecast by all members, indicating a lower forecast uncertainty than during the locally triggered convection situation several hours earlier.

This qualitative impression of the performance of the COSMO-DE-EPS forecasts during COPS IOP15 is confirmed applying different quality measures (Fig. 3). The time series of the conventional score FBI highlights (i) the gross underestimation of the forecast rainfall, (ii) the better performance of members 1, 6, 11 and 16 (indicated with solid lines in Fig. 3a) during the late afternoon hours between 1715 and 2115 UTC, (iii) the failure of the other ensemble members to forecast precipitation during that period (FBI < 0.1), and (iv) the increase in forecast quality of those other members from 2115 UTC onwards when the forced-frontal precipitation is entering the COPS area. Application of DAS confirms the better performance of the four members with the modified entrainment rate during the triggered convection situation (Fig. 3b, note that DAS is negatively oriented, i.e. the lower the better). Overall, the time series of DAS shows greater variability since not only the amplitude error (as in FBI) but also the location error is considered.

Seen by another perspective, the differences in forecast quality during the distinct atmospheric regimes on 12 August can be depicted using a scatter diagram (Fig. 4) showing the mean FBI of the forecasts of any group (employing the same lateral boundary conditions or the same physical perturbation) versus its standard deviation (called spread FBI in the following). The spread FBI is normalized with the mean FBI to discern the relative variability of the individual members within one group. In this skill-spread relationship a clear separa-

tion between both situations becomes evident: during the triggered convection regime (1215 to 2115 UTC) the mean FBI is generally low (FBI < 0.2) with a large spread FBI, since most of the ensemble members fail to produce precipitation except the group comprising members 1, 6, 11 and 16. On the other hand, during the forced-frontal regime (2215 to 2315 UTC) the mean FBI is higher (0.2 < FBI < 0.5) and the spread is smaller (spread FBI < 0.5), since all ensemble members predict rainfall. One exception to this pattern is found, namely that the mean and spread FBI resulting from the four (best) members 1, 6, 11 and 16 between 1715 and 2115 UTC show a high mean FBI with a low spread FBI (see previous discussion, Fig. 3a).

Leaving the 12 August we now examine the entire period from 8 to 16 August by applying the convective adjustment time scale, a diagnostic tool to discriminate between the triggered convection regime governed by local processes and the forced-frontal regime governed by synoptic-scale disturbances. During the nine day period COSMO-DE-EPS is available, different flow regimes prevailed in the COPS region. In Figure 5 the time series of the mean precipitation in conjunction with the mean convective time scale averaged over the 360 x 360 km^2 COPS region is displayed. The period can be split in different episodes: from 8 to 10 August the situation is dominated by strong precipitation intensities and small convective time scales due to a prevailing upper-level trough across central Europe leading to an easterly flow in the COPS region. On 11 August the flow pattern changed and the next 3 days (12–14 August) are characterized by small mean precipitation amounts and a predominantly large mean convective time scale indicating weakly forced conditions at the synoptic scale. However, as discussed previously, a short-term forced-frontal situation occurred in the night from 12 to 13 August indicated by a short-lived decrease in the convective time scale. On the last two days (15 and 16 August) the meteorological conditions were predominantly governed by synoptic-scale disturbances crossing the COPS region. Overall, the prevailing flow condition during the period is the synoptically forced regime classified 87 hours compared to 21 hours based on a threshold value of the convective time scale of 6 hours (in the residual hours τ_c could not be computed due to the absence of rain).

The behaviour of the mean FBI and its spread is condensed in Figure 6 showing the skill-spread relationship for the entire period. Here, the convective time scale is used to stratify the data points into locally forced situations ($\tau_c > 6$ h) and forced-frontal situations ($\tau_c < 6$ h). Overall, both flow regimes can be separated fairly well. Again, during the locally forced regime the mean FBI is characterized by low mean FBI (FBI < 0.3) and high spread FBI. On the other hand, the synoptically forced regime is characterized by higher mean FBI and lower spread FBI. The average values of skill and spread of
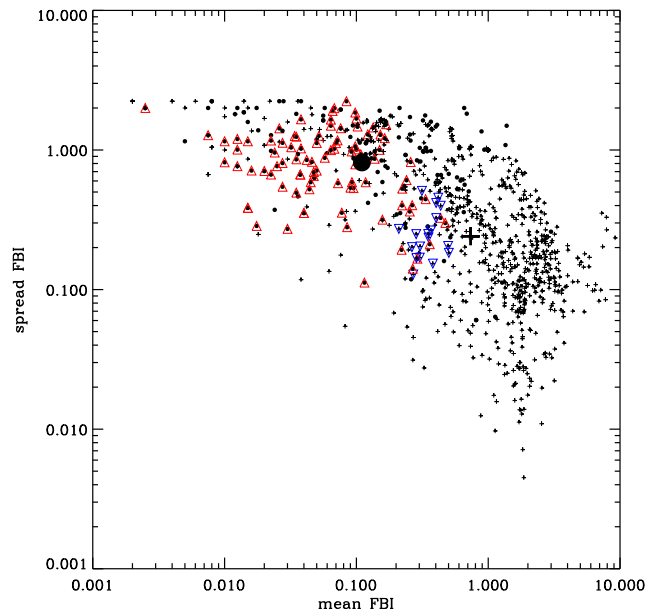

Figure 6: Skill-spread relationship of the entire period (as in Fig. 4, but on a log-log scale) stratified by convective time scale. The filled circles denote the values when the convective time scale is larger than 6 hours indicating the triggered convection regime, the plus signs the values when the time scale is less than 6 hours indicating equilibrium conditions governed by synoptic-scale forcing. The fat symbols represent the mean of both regimes. Additionally, the red upward triangles highlight values for 12 August and a time scale larger 6 hours, while the blue downward triangles the values on that day when the time scale is less than 6 hours.

both regimes are clearly separated (Fig. 6, average skill (spread) 0.11 (0.81) during triggered regime versus 0.74 (0.24) during forced-frontal regime).

Seen by the convective time scale perspective, we revisit the meteorological interesting conditions including the regime change on 12 August. These data points are highlighted in Figure 6. Although the scatter diagrams (Figs. 4 and 6) differ in scale (linear versus log-log-scale) one can easily confirm the good agreement classifying both regimes based on visual inspection and scores on the one hand (Fig. 4) and the convective time scale on the other hand (Fig. 6). During the late afternoon triggered convection conditions prevailed, characterized by a strong sensitivity on the physical perturbation, and hence showing a large forecast uncertainty (low mean FBI and large spread FBI, Fig. 4). This is confirmed by the convective time scale attaining values larger than 6 hours, as is typical for locally forced, triggered convection meteorological regimes (upward triangles in Fig. 6). In the late evening and at night the approaching surface cold front accompanied by precipitation causes a regime change. Now, the rainfall is less sensitive to the physical perturbations, that is, the precipitation forecast exhibits a smaller uncertainty, and the convective time scale attains values less than 6 hours, typical for synoptically-forced situations (downward triangles).

4　Conclusions

Forcasts of the convection-permitting COSMO-DE-EPS system allow for an examination of the forecast uncertainty of convective precipitation during a nine day period during the COPS field campaign in August 2007. Two distinct meteorological regimes can be distinguished depending on the control of convection as measured by the mean and spread FBI and the convective adjustment time scale. Firstly, during triggered convection situations the precipitation forecast of COSMO-DE-EPS reacts sensitively to changes in the model physics (as shown for the regime change on 12 August), and the convective time scale attains values of more than a few hours (here a threshold of 6 hours was selected). Convective precipitation is primarily governed by local processes like orography or boundary layer phenomena leading to a large forecast uncertainty. Secondly, during forced-frontal convection situations, the precipitation is controlled by synoptic forcing that is determining the creation of instability. This regime is characterized by short convective time scales.

Currently a re-forecasting project using the COSMO-DE-EPS for the entire summer 2009 is underway at DWD. It is planned to apply the presented methodology on this large data set. In future it is planned to examine the potential of the convective adjustment time scale as a quantity to construct a flow-dependent convection-permitting EPS directed towards adaptive ensemble modeling.

Acknowledgments

References

ARAKAWA, A, W.H. SCHUBERT, 1974: Interaction of a cumulus cloud ensemble with the large-scale environment Part I. – J. Atmos. Sci. **31**, 674–701.

BALDAUF, M., K. STEPHAN, S. KLINK, C. SCHRAFF, A. SEIFERT, J. FOERSTNER, T. REINHARDT, C.J. LENZ, 2006: The new very short range forecast model LM-K for the convection-resolving scale. – Second THORPEX International Science Symposium. Extended Abstracts, Part B, 148–149, available online at www.pa.op.dlr.de/stiss/proceedings.html.

DONE, J.M., G. C. CRAIG, S.L. GRAY, P.A. CLARK, M.E.B. GRAY, 2006: Mesoscale simulations of organized convection: Importance of convective equilibrium. – Quart. J. Roy. Meteor. Soc. **132**, 737–756.

GEBHARDT, C., S.E. THEIS, M. PAULAT, Z. BEN BOUAL-LEGUE, 2010: Uncertainties in COSMO-DE precipitation forecasts introduced by model perturbations and variation of lateral boundaries. – Atmos. Res., published online, DOI:10.1016/j.atmosres.2010.12.008.

EBERT, E.E., U. DAMRATH, W. WERGEN, M.E. BALDWIN, 2003: The WGNE assessment of short-term quantitative precipitation forecasts. – Bull. Amer. Meteor. Soc. **84**, 481–492.

JONES, M.S., B.A. COLLE, J.S. TONGUE, 2007: Evaluation of a mesoscale short-range ensemble forecast system over the North-East United States. – Wea. Forecast. **22**, 36–55.

KALNAY, E., 2003: Atmospheric Modeling, Data Assimilation, and Predictability.– Cambridge University Press, 341 pp.

KEIL, C., G.C. CRAIG, 2009: A displacement and amplitude score employing an optical flow technique. – Wea. Forecast. **24**, 1297–1308.

KONG, F., K.K. DROEGEMEIER, N.L. HICKMON, 2006: Multi-resolution ensemble forecasts of an observed tornadic thunderstorm system. Part I: Comparison of coarse- and fine-grid experiments. – Mon. Wea. Rev. **134**, 807–833.

LEUTBECHER, M., T.N. PALMER, 2008: Ensemble forecasting. – J. Comp. Phys. **227**, 3515–3539.

MARSIGLI, C., A. MONTANI, T. PACCAGNELLA, 2008: The COSMO-SREPS ensemble for short-range system: analysis and verification on the MAP D-PHASE DOP. – Joint MAP D- PHASE Scientific Meeting – COST 731 mid term seminar, 19–22 May 2008, Bologna, Italy 9–14.

MOLINARI, J., M. DUDEK, 1992: Parameterization of convective precipitation in mesoscale numerical models: A critical review. – Mon. Wea. Rev. **120**, 326–344.

MOLINI, L., A. PARODI, N. REBORA, G.C. CRAIG, 2011: Classifying severe rainfall events over Italy by hydrometeorological and dynamical criteria. – Quart. J. Roy. Meteor. Soc. **137**, 148–154.

MOLTENI, F., R. BUIZZA, T. N. PALMER, T. PETROLIAGIS, 1996: The ECMWF ensemble prediction system: Methodology and validation. – Quart. J. Roy. Meteor. Soc. **122**, 73–119.

WEUSTHOFF, T., D. LEUENBERGER, C. KEIL, G.C. CRAIG, 2011: Best member selection for convective-scale ensembles. – Meteorol. Z. **20**, 153–164.

WILKS , D.S., 2006: Statistical methods in the atmospheric sciences. – Academic Press, New York, 628 pp.

WULFMEYER, V., A. BEHRENDT, H. BAUER, C. K. U. CORSMEIER, A. BLYTH, G.C. CRAIG, U. SCHUMANN, M. HAGEN, S. CREWELL, P.D. GIROLAMO, C. FLAMANT, M. MILLER, A. MONTANI, S. MOBBS, E. RICHARD, M. ROTACH, M. ARPAGAUS, H. RUSSCHENBERG, P. SCHLÜSSEL, M. KÖNIG, V. GARTNER, R. STEINACKER, M. DORNIGER, D. TURNER, T. WECKWERTH, A. HENSE, C. SIMMER, 2008: The Convective and Orographically induced Precipitation Study: A Research and Development Project of the World Weather Research Program for improving quantitative precipitation forecasting in low-mountain regions. – Bull. Amer. Meteor. Soc. **89**, 1477–1486.

ZIMMER, M., G.C. CRAIG , C. KEIL, H. WERNLI, 2011: Classification of precipitation events with a convective response timescale and their forecasting characteristics. – Geophys. Res. Lett. **38**, L05802.